

This is a repository copy of *UAV-Mounted RIS Enabled Maritime Secure Sensing With Joint Beamforming and Trajectory Design*.

White Rose Research Online URL for this paper:

<https://eprints.whiterose.ac.uk/id/eprint/226511/>

Version: Accepted Version

Article:

Hao, Xu, Ma, Haoyu, Wang, Wei et al. (3 more authors) (2025) UAV-Mounted RIS Enabled Maritime Secure Sensing With Joint Beamforming and Trajectory Design. IEEE Transactions on Vehicular Technology. ISSN 0018-9545

<https://doi.org/10.1109/TVT.2025.3565951>

Reuse

This article is distributed under the terms of the Creative Commons Attribution (CC BY) licence. This licence allows you to distribute, remix, tweak, and build upon the work, even commercially, as long as you credit the authors for the original work. More information and the full terms of the licence here:

<https://creativecommons.org/licenses/>

Takedown

If you consider content in White Rose Research Online to be in breach of UK law, please notify us by emailing eprints@whiterose.ac.uk including the URL of the record and the reason for the withdrawal request.

UAV-Mounted RIS Enabled Maritime Secure Sensing With Joint Beamforming and Trajectory Design

Xu Hao, Haoyu Ma, Wei Wang, *Member, IEEE*, Feng Zeng, Kanapathippillai Cumanan, *Senior Member, IEEE*, and Emil Björnson, *Fellow, IEEE*

Abstract—This paper considers a challenging maritime secure sensing system, in which, a legitimate shipborne radar L needs to detect in real-time the state of a collaborative unmanned aerial vehicle (UAV) in the presence of an illegitimate or unauthorized shipborne radar U. To address this challenge, we propose a novel UAV-mounted reconfigurable intelligent surface (RIS) assisted approach, where the RIS is mounted on the UAV for enhancing/suppressing its reflected signal towards the L/U to facilitate/prevent its detection of the UAV. Furthermore, the UAV target can also adjust its flight route to move closer to/away from the L/U to improve/decrease the sensing performance. Due to the mobility of both the shipborne radars and UAVs, the Doppler shift effects of the RIS-ship channel need to be considered. In such a setup, the maximization of the received power at the L is formulated into an optimization problem while suppressing the received power at the U below a certain threshold by jointly designing the reflecting phase shifts of RIS and the 3D flight trajectory of UAV. The non-convex optimization problem is decomposed into two subproblems and solved via an iterative algorithm. Simulation results are presented to corroborate the effectiveness and tremendous potential of UAV-mounted RISs in the maritime secure sensing.

Index Terms—Maritime sensing security, UAV-mounted RIS, trajectory design, passive beamforming.

I. INTRODUCTION

Recently, unmanned aerial vehicles (UAVs) have been applied to various maritime activities due to their on-demand deployment and flexible dispatch [1]–[3]. However, the physical characteristics of these legitimate UAVs (e.g., location and velocity) may be detected by the unauthorized radar due

to the wide field of line-of-sight on the sea. Hence, various secure sensing techniques have been proposed to address this issue, such as designing specific shapes [4], wrapping stealth materials [5] and installing radar jammers [6]. Although the above methods can significantly reduce the probability of detection by the illegitimate radar, they will also inevitably make the target invisibility to any legitimate radar.

Unlike the conventional secure sensing schemes, reconfigurable intelligent surfaces (RIS), also referred to as intelligent reflecting surfaces (IRS), have been applied to improve the wireless sensing performance by reconfiguring the propagation environment [7]–[9]. For instance, an RIS-assisted MIMO radar detection problem was first investigated in [10], where the RIS can boost the reflected signals and suppress the malicious interference. This RIS-aided wireless sensing was then extended to a multiple target sensing scenario in [11]. The authors in [12] studied using RIS in the integrated sensing and communication (ISAC) for further improving the target detection capability. In [13], the authors investigated an RIS-aided ISAC network with multiple targets and users, where the RIS was used to support both sensing and communicating in a cluttered environment. Moreover, the authors in [14] introduced the RIS to the secure ISAC network and leveraged its passive beamforming gain to enhance the sensing performance.

However, the aforementioned works only assumed that the RIS is used as additional anchor [10]–[14], which may not achieve a better detection performance when the radar cross section of the target is limited. More importantly, it is generally challenging to deploy the RIS at the appropriate location in oceans. Recently, an interesting target-mounted RIS approach was proposed in [15], [16], where the RIS is mounted on the target to directly control the signal reflection. In [15], the authors considered mounting the RIS on the sensing target to estimate its position and direction information. Further, this target-mounted RIS was extended to the secure sensing scenario in [16], where the RIS is installed on the target's surface to control its reflected signal towards the legitimate or illegal radar. However, the works in [10]–[16] only considered terrestrial environments, which may not be applicable to maritime wireless sensing scenarios. This is because the radars in the maritime, unlike them on the terrestrial settings with static deployments and random distributions, are typically installed on ships, which often move on predefined lanes to avoid collision. Moreover, in contrast to the terrestrial stationary target, the maritime mobile target (e.g. UAV) can

Copyright (c) 20xx IEEE. Personal use of this material is permitted. However, permission to use this material for any other purposes must be obtained from the IEEE by sending a request to pubs-permissions@ieee.org.

Xu Hao, Haoyu Ma, Wei Wang and Feng Zeng are with the School of Information Science and Technology, Nantong University, Nantong 226019, China (e-mail: 2330310012@stmail.ntu.edu.cn, 2330310040@stmail.ntu.edu.cn, wwang2011@ntu.edu.cn, zengfeng@ntu.edu.cn).

Kanapathippillai Cumanan is with the School of Physics, Engineering and Technology, University of York, York YO10 5DD, U.K. (e-mail: kanapathippillai.cumanan@york.ac.uk).

Emil Björnson is with the School of Electrical Engineering and Computer Science, KTH Royal Institute of Technology, Stockholm 16440, Sweden (e-mail: emilbj@kth.se).

The work of X. Hao and W. Wang were supported in part by the Key Research and Development Program of Jiangsu Province under Grant BE2021013-1 and in part by the Postgraduate Research & Practice Innovation Program of School of Information Science and Technology, Nantong University under Grant NTUSISTPR24_02. The work of K. Cumanan was supported by the UK Engineering and Physical Sciences Research Council (EPSRC) under Grant number EP/X01309X/1. The work of E. Björnson was supported by the Vinnova through the SweWIN center under Grant number 2023-00572. (*Corresponding author: Wei Wang*)

further improve/reduce the sensing accuracy by designing its trajectory. Motivated by the aforementioned challenges, this paper studies a new maritime secure sensing system, in which, a legitimate shipborne radar L needs to detect in real-time the state of a collaborative UAV in the presence of an unauthorized shipborne radar U.¹ In particular, the mobility of both shipborne radars and UAVs are also considered. To tackle this challenge, we propose a UAV-mounted RIS enabled approach, where the RIS is deployed on the collaborative UAV to enhance the received signal at the L receiver and suppress it at the U receiver. Our objective is to jointly design the RIS's reflecting phase shifts and the UAV's flight trajectory for maximizing the received power at the L while suppressing that at the U below a certain level. The main contributions are summarized as follows:

- 1) We propose a new maritime secure sensing model by mounting the RIS on the collaborative UAV. Additionally, we consider the impact of Doppler shifts in the RIS-ship channel and investigate the joint beamforming and trajectory optimization to achieve secure detection of the UAV.
- 2) We formulate an optimization problem to maximize the received power at the L while suppressing that at the U below a certain threshold. Then, we decompose the considered problem into two subproblems and derive numerical solutions of the reflecting phase shifts and 3D flight trajectory.
- 3) Finally, we provide the complexity analysis and verify the effectiveness of the proposed scheme. Furthermore, we demonstrate that for the maritime mobile sensing, the proposed UAV-mounted RIS-aided design achieves a significant secure sensing gain compared to the terrestrial scheme.

Notations: Boldface lowercase and uppercase letters denote vectors and matrices, respectively. $(\cdot)^H$, $\|\cdot\|$, $|\cdot|$, $\text{rank}(\cdot)$ and $\text{tr}(\cdot)$ represent the conjugate transpose, Euclidean norm, absolute value, matrix rank and trace, respectively. Moreover, $\arg(\cdot)$ represents the component-wise phase of a complex vector, $\mathcal{CN}(0, \sigma^2)$ denotes the complex Gaussian distribution with zero mean and σ^2 variance, and $\mathbf{A} \succeq 0$ indicates the positive semidefinite matrix, respectively.

II. SYSTEM MODEL AND PROBLEM FORMULATION

As shown in Fig. 1, we consider a maritime secure sensing system assisted by the UAV target-mounted RIS, where both the shipborne radars L and U intend to detect the same UAV target by sending radar pulses. Specifically, the RIS is mounted on the UAV to control its signal reflection to the L and U, where L/U are assumed to move along pre-planned trajectories.² It is assumed that the L/U are equipped with M_L/M_U antennas, while the RIS consists of M reflecting elements. Furthermore, we assume that there is no direct link between the shipborne radars L and U, due to the sea

¹This system setting has a number of potential applications in UAV-aided maritime activities, where the UAV needs to keep the visible state to the legitimate radar while preventing the detection by the unauthorized radar.

²This is typical for ocean scenarios [1]–[3], where all ships have fixed routes to avoid collision.

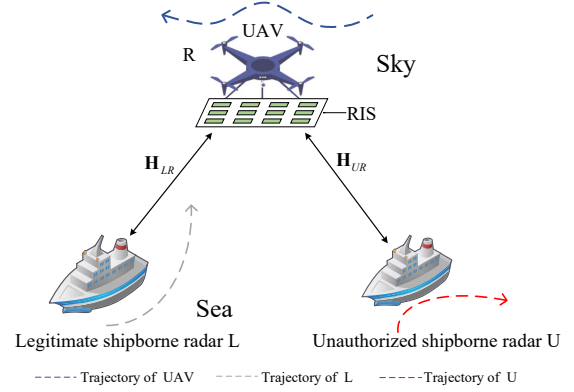


Fig. 1: UAV-mounted RIS enabled maritime secure sensing system.

wave movement or existence of other ships. Let T denotes the UAV flight time and $d_t = T/N$ represents the equal time slots, where $\mathcal{N} \triangleq \{1, 2, \dots, N\}$. Moreover, let the coordinates $(\mathbf{q}_l[n], 0)$, $\mathbf{q}_l[n] = (x_l[n], y_l[n])$, and $(\mathbf{q}_u[n], 0)$, $\mathbf{q}_u[n] = (x_u[n], y_u[n])$ represent the positions of the L and U respectively. In addition, we denote the UAV R coordinates as $(\mathbf{q}_r[n], h_r[n])$, where $\mathbf{q}_r[n] = (x_r[n], y_r[n])$. Accordingly, for any $n \in \mathcal{N}$, the UAV's mobility constraints can be formulated as

$$\|\mathbf{q}_r[n] - \mathbf{q}_r[n-1]\| \leq V_{r,h} d_t, \quad (1a)$$

$$|h_r[n] - h_r[n-1]| \leq V_{r,v} d_t, \quad (1b)$$

$$h_s \leq h_r[n] \leq h_l, \quad (1c)$$

where $V_{r,h}$ and $V_{r,v}$ denote the maximum horizontal and vertical speed, and h_l and h_s represent the maximum and minimum flight altitudes of the UAV, respectively.

Note that the UAV target R and shipborne radars L/U are mobile in the maritime, thus the Doppler shift effects of the RIS-ship channel need to be considered. The channel coefficients at time n are defined as

$$\mathbf{G}_{iRj}[n] = \mathbf{H}_{jR}^T[n] \Phi[n] \mathbf{H}_{iR}[n], \quad (2)$$

where $\mathbf{H}_{iR}[n] = \frac{\sqrt{\beta_0}}{d_{iR}[n]} e^{j\theta_i[n]} e^{H(\phi_i[n], M_i)}$, $e^{j\theta_i[n], M_i} = \left[1, e^{-j\frac{2\pi d}{\lambda} \phi_i[n]}, \dots, e^{-j\frac{2\pi d}{\lambda} (M_i-1) \phi_i[n]} \right]^T$ and $\phi_i[n] = \frac{x_r[n] - x_i[n]}{d_{iR}[n]}$, $i, j \in \{L, U\}$. The symbols β_0 , λ , d and d_{iR} represent the reference power gain, the carrier wavelength, the antenna separation and the corresponding distances, respectively. Moreover, the symbols $\Phi[n] = \text{diag}(e^{j\theta_1[n] + 2\pi n f_{D1j}}, \dots, e^{j\theta_M[n] + 2\pi n f_{DMj}})$ denotes the RIS reflection coefficients, $f_{Dij} = \frac{V_r}{\lambda} \phi_i[n] + \frac{V_j}{\lambda} \phi_j[n]$ represents the Doppler terms, and V_r and V_j indicate the speeds of the UAV and shipborne radars, respectively.

Based on this channel model, we assume that both shipborne radars L and U transmit one coherent burst of K_p nonconsecutive radar pulses with a constant pulse repetition interval, denoted as T_p , to detect the UAV target. When the signals from L and U are overlapped at the RIS, the received

signal at the L/U receiver can be expressed as³

$$y_i[n] = \boldsymbol{\omega}_i^T \mathbf{G}_{iRi}[n] \boldsymbol{\omega}_i x_i[n] + \boldsymbol{\omega}_i^T \mathbf{G}_{jRi}[n] \boldsymbol{\omega}_j x_j[n] + n_i[n], \quad (3)$$

where $x_i[n] = \sqrt{P_i} p_i[n]$, $i, j \in \{L, U\}$, $i \neq j$. Here, P_i and $p_i[n]$ represent the transmit powers and the corresponding radar pulses with normalized power, respectively. The symbols $\boldsymbol{\omega}_i \in \mathbb{C}^{M_i \times 1}$ and $n_i[n] \sim \mathcal{CN}(0, \sigma_i^2)$ indicate the corresponding transmit beamformers and the noise signals, respectively.

In practice, the performance of target detection/estimation improves with the increase of received signal power [16]. Thus, we use the received power at the L/U as the performance metric to evaluate the effectiveness of UAV-mounted RIS aided secure sensing. According to (2) and (3), the received powers at the L and U are respectively given by

$$Q_L[n] = P_{LRL} |g_{LRL}[n]|^2 + P_{URL} |g_{URL}[n]|^2, \quad (4a)$$

$$Q_U[n] = P_{URU} |g_{URU}[n]|^2 + P_{LRU} |g_{LRU}[n]|^2, \quad (4b)$$

where $P_{iRj} = P_i |e^H(\phi_i[n], M_i) \boldsymbol{\omega}_i|^2 |e^H(\phi_j[n], M_j) \boldsymbol{\omega}_j|^2$. $g_{iRj}[n] = \mathbf{h}_{jR}^T[n] \boldsymbol{\Phi}[n] \mathbf{h}_{iR}[n]$ and $\mathbf{h}_{iR}[n] = \frac{\sqrt{\beta_0}}{d_{iR}[n]} e(\phi_i[n], M)$, $i, j \in \{L, U\}$.

Under the above setting, we are interested in maximizing the average received power \bar{Q}_L while suppressing the received power $Q_U[n]$ below a certain threshold, by jointly designing the RIS reflection coefficients, $\boldsymbol{\Phi}[n]$, and the UAV flight trajectory, $\{\mathbf{q}_r[n], h_r[n]\}$. Here, the constraints include the UAV's mobility constraint, the RIS's phase shifts constraint, and the secure sensing constraint for U. Therefore, we formulate the optimization problem as

$$\begin{aligned} & \underset{\{\mathbf{q}_r[n], h_r[n]\}, \boldsymbol{\Phi}[n]}{\text{maximize}} && \frac{1}{N} \sum_{n=1}^N Q_L[n] \\ & \text{s.t.} && (1a) \sim (1c), \\ & && Q_U[n] \leq \gamma, \\ & && \|\boldsymbol{\omega}_i\|^2 \leq 1, i \in \{L, U\}, \\ & && 0 \leq \theta_m[n] \leq 2\pi, \forall m, n, \end{aligned} \quad (5)$$

where γ represents the given received power threshold for U.

Since the variables $\boldsymbol{\Phi}[n]$ and $\{\mathbf{q}_r[n], h_r[n]\}$ are coupled in $Q_L[n]$ and $Q_U[n]$, it is highly complicated to determine the global optimal solution for problem (5). Thus, to circumvent this non-convexity dilemma, an alternating optimization is proposed to yield a feasible solution for problem (5).

III. PROPOSED JOINT DESIGN SCHEME

In this section, an iterative optimization scheme is developed by alternately optimizing the RIS beamforming matrix and UAV 3D trajectory to solve the problem (5).

³The proposed design can be readily extended to the received signal only from L or U case, which is discussed in the simulation results.

A. Optimization of RIS's phase-shift matrix $\boldsymbol{\Phi}[n]$

With any given $\{\mathbf{q}_r[n], h_r[n]\}$, the maximum-ratio transmission is the optimal beamforming scheme [11], i.e., $\boldsymbol{\omega}_L^* = \frac{e(\phi_L[n], M_L)}{\sqrt{M_L}}$ and $\boldsymbol{\omega}_U^* = \frac{e(\phi_U[n], M_U)}{\sqrt{M_U}}$. Thus, by substituting $\boldsymbol{\omega}_L^*$ and $\boldsymbol{\omega}_U^*$ to (5), the original non-convex problem reduces to the following form :

$$\begin{aligned} & \underset{\theta[n]}{\text{maximize}} && \frac{1}{N} \sum_{n=1}^N P_{LRL}^* |g_{LRL}[n]|^2 + P_{URL}^* |g_{URL}[n]|^2 \\ & \text{s.t.} && P_{URU}^* |g_{URU}[n]|^2 + P_{LRU}^* |g_{LRU}[n]|^2 \leq \gamma, \\ & && 0 \leq \theta_m[n] \leq 2\pi, \forall m, n, \end{aligned} \quad (6)$$

where $P_{iRj}^* = P_i |e^H(\phi_i[n], M_i) \boldsymbol{\omega}_i^*|^2 |e^H(\phi_j[n], M_j) \boldsymbol{\omega}_j^*|^2 = P_i M_i M_j$, $i, j \in \{L, U\}$.

We first introduce a new variable $\mathbf{k}[n] = [k_1, \dots, k_M]^H$, where $k_m = e^{j\theta_m[n]}$, $\forall m$. Then, we transform the following variables into their equivalent forms as

$$|g_{LRL}[n]| = |\mathbf{h}_{LR}^T[n] \boldsymbol{\Phi}[n] \mathbf{h}_{LR}[n]| = \mathbf{k}^H[n] \mathbf{A}_1, \quad (7a)$$

$$|g_{URL}[n]| = |\mathbf{h}_{LR}^T[n] \boldsymbol{\Phi}[n] \mathbf{h}_{UR}[n]| = \mathbf{k}^H[n] \mathbf{A}_2, \quad (7b)$$

$$|g_{URU}[n]| = |\mathbf{h}_{UR}^T[n] \boldsymbol{\Phi}[n] \mathbf{h}_{UR}[n]| = \mathbf{k}^H[n] \mathbf{A}_3, \quad (7c)$$

$$|g_{LRU}[n]| = |\mathbf{h}_{UR}^T[n] \boldsymbol{\Phi}[n] \mathbf{h}_{LR}[n]| = \mathbf{k}^H[n] \mathbf{A}_4, \quad (7d)$$

where $\mathbf{A}_1 = \text{diag}(\mathbf{h}_{LR}^T[n] \mathbf{h}_{LR}[n])$, $\mathbf{A}_2 = \text{diag}(\mathbf{h}_{LR}^T[n] \mathbf{h}_{UR}[n])$, $\mathbf{A}_3 = \text{diag}(\mathbf{h}_{UR}^T[n] \mathbf{h}_{UR}[n])$, $\mathbf{A}_4 = \text{diag}(\mathbf{h}_{UR}^T[n] \mathbf{h}_{LR}[n])$. Thus, problem (6) is recast as

$$\begin{aligned} & \underset{\mathbf{k}[n]}{\text{maximize}} && \frac{1}{N} \sum_{n=1}^N P_{LRL}^* \mathbf{k}^H[n] \mathbf{A}_1 \mathbf{A}_1^H \mathbf{k}[n] + P_{URL}^* \mathbf{k}^H[n] \mathbf{A}_2 \mathbf{A}_2^H \mathbf{k}[n] \\ & \text{s.t.} && P_{URU}^* \mathbf{k}^H[n] \mathbf{A}_3 \mathbf{A}_3^H \mathbf{k}[n] + P_{LRU}^* \mathbf{k}^H[n] \mathbf{A}_4 \mathbf{A}_4^H \mathbf{k}[n] \leq \gamma, \\ & && |k_m[n]| = 1, \forall m, n. \end{aligned} \quad (8)$$

Then, by letting $\mathbf{B}_1 = P_{LRL}^* \mathbf{A}_1 \mathbf{A}_1^H + P_{URL}^* \mathbf{A}_2 \mathbf{A}_2^H$ and $\mathbf{B}_2 = P_{URU}^* \mathbf{A}_3 \mathbf{A}_3^H + P_{LRU}^* \mathbf{A}_4 \mathbf{A}_4^H$, problem (8) can be rewritten as

$$\begin{aligned} & \underset{\mathbf{k}[n]}{\text{maximize}} && \frac{1}{N} \sum_{n=1}^N \mathbf{k}^H[n] \mathbf{B}_1 \mathbf{k}[n] \\ & \text{s.t.} && \mathbf{k}^H[n] \mathbf{B}_2 \mathbf{k}[n] \leq \gamma, \\ & && |k_m[n]| = 1, \forall m, n. \end{aligned} \quad (9)$$

However, the problem in (9) is NP-hard in general [17]. Note that $\mathbf{k}^H[n] \mathbf{B}_1 \mathbf{k}[n] = \text{tr}(\mathbf{B}_1 \mathbf{k}[n] \mathbf{k}^H[n])$ and $\mathbf{k}^H[n] \mathbf{B}_2 \mathbf{k}[n] = \text{tr}(\mathbf{B}_2 \mathbf{k}[n] \mathbf{k}^H[n])$, by defining $\mathbf{K}[n] = \mathbf{k}[n] \mathbf{k}^H[n]$ and removing $\text{rank}(\mathbf{K}[n]) = 1$, we relax problem (9) into the following form:

$$\begin{aligned} & \underset{\mathbf{K}[n]}{\text{maximize}} && \frac{1}{N} \sum_{n=1}^N \text{tr}(\mathbf{B}_1 \mathbf{K}[n]) \\ & \text{s.t.} && \text{tr}(\mathbf{B}_2 \mathbf{K}[n]) \leq \gamma, \\ & && |\mathbf{K}[n]_{m,m}| = 1, \forall m, n, \\ & && \mathbf{K}[n] \succeq 0. \end{aligned} \quad (10)$$

Problem (10) is a standard semidefinite program, which can be solved efficiently by CVX [18]. However, the optimal solution $\mathbf{K}^*[n]$ of problem (10) is not always guaranteed to be rank-one. As such, we can leverage the Gaussian randomization to recover a feasible solution [13], [17]. Then, the approximate solution to problem (9) can be derived as

$$\mathbf{k}^*[n] = e^{j \arg(\mathbf{r})}, \quad (11)$$

where $\mathbf{r} \sim \mathcal{CN}(0, \mathbf{K}^*[n])$ denotes the Gaussian randomization vectors.

B. Optimization of the UAV's flight trajectory $\{\mathbf{q}_r[n], h_r[n]\}$

For given $\Phi[n]$ from (11), the received power at the L and U are respectively expressed as

$$Q_L^*[n] = P_{LRL}^* \frac{D_1^2}{d_{LR}^4[n]} + P_{URL}^* \frac{D_2^2}{d_{LR}^2[n]d_{UR}^2[n]}, \quad (12a)$$

$$Q_U^*[n] = P_{URU}^* \frac{D_3^2}{d_{UR}^4[n]} + P_{LRU}^* \frac{D_4^2}{d_{LR}^2[n]d_{UR}^2[n]}, \quad (12b)$$

where $D_1 = \beta_0 |\mathbf{e}^T(\phi_L[n], M)\Phi[n]\mathbf{e}(\phi_L[n], M)|$, $D_2 = \beta_0 |\mathbf{e}^T(\phi_L[n], M)\Phi[n]\mathbf{e}(\phi_U[n], M)|$, $D_3 = \beta_0 |\mathbf{e}^T(\phi_U[n], M)\Phi[n]\mathbf{e}(\phi_U[n], M)|$ and $D_4 = \beta_0 |\mathbf{e}^T(\phi_U[n], M)\Phi[n]\mathbf{e}(\phi_L[n], M)|$. Thus, problem (5) can be recast as

$$\begin{aligned} & \underset{\{\mathbf{q}_r[n], h_r[n]\}}{\text{maximize}} \quad \frac{1}{N} \sum_{n=1}^N Q_L^*[n] \\ & \text{s.t.} \quad Q_U^*[n] \leq \gamma, \\ & \quad (1a) \sim (1c). \end{aligned} \quad (13)$$

Note that the problem (13) is challenging to be directly solved since the variables $\{\mathbf{q}_r[n], h_r[n]\}$ are coupled in $Q_L^*[n]$ and $Q_U^*[n]$. To tackle it, based on (12a) and (12b), by introducing slack variables $s_1[n]$, $s_2[n]$, problem (13) is equivalently transformed as

$$\begin{aligned} & \underset{\{\mathbf{q}_r[n], h_r[n], s_1[n], s_2[n]\}}{\text{maximize}} \quad \frac{1}{N} \sum_{n=1}^N \frac{P_{LRL}^* D_1^2}{s_1^2[n]} + \frac{P_{URL}^* D_2^2}{s_1[n]s_2[n]} \\ & \text{s.t.} \quad C1: \|\mathbf{q}_r[n] - \mathbf{q}_l[n]\|^2 + |h_r[n]|^2 \geq s_1[n], \\ & \quad C2: \|\mathbf{q}_r[n] - \mathbf{q}_u[n]\|^2 + |h_r[n]|^2 \geq s_2[n], \\ & \quad C3: s_i[n] \geq h_s, i \in \{1, 2\}, \\ & \quad C4: \frac{P_{URU}^* D_3^2}{s_2^2[n]} + \frac{P_{LRU}^* D_4^2}{s_1[n]s_2[n]} \leq \gamma, \\ & \quad (1a) \sim (1c). \end{aligned} \quad (14)$$

Then, by the first-order Taylor approximation, the objective function in problem (14) can be rewritten as

$$\begin{aligned} \frac{P_{LRL}^* D_1^2}{s_1^2[n]} + \frac{P_{URL}^* D_2^2}{s_1[n]s_2[n]} & \geq t_1^l[n] + t_2^l[n] - \frac{t_2^l[n]}{s_2^l[n]}(s_2[n] - s_2^l[n]) \\ & \quad - \frac{(2t_1^l[n] + t_2^l[n])}{s_1^l[n]}(s_1[n] - s_1^l[n]), \end{aligned} \quad (15)$$

Algorithm 1 Proposed Joint Design Scheme for (5)

Initialize $\{\mathbf{q}_r^0[n], h_r^0[n]\}$, $\Phi^0[n]$, Q_L^0 , ϵ and $l = 1$.

Repeat

Obtain $\{\mathbf{q}_r^l[n], h_r^l[n]\}$ to (17) for any given $\Phi^{(l-1)}[n]$.

Update $\Phi^l[n]$ by using (11) under given $\{\mathbf{q}_r^l[n], h_r^l[n]\}$.

Determine Q_L^l based on $\{\mathbf{q}_r^l[n], h_r^l[n]\}$ and $\Phi^l[n]$.

Let $l = l + 1$.

Until $|Q_L^l - Q_L^{(l-1)}| < \epsilon$.

Output: $\{\mathbf{q}_r^l[n], h_r^l[n]\}$, $\Phi^l[n]$ and Q_L^l .

where $t_1^l[n] = \frac{P_{LRL}^* D_1^2}{(s_1^l[n])^2}$ and $t_2^l[n] = \frac{P_{URL}^* D_2^2}{s_1^l[n]s_2^l[n]}$, and $s_1^l[n]$ and $s_2^l[n]$ represent the l -th feasible solutions. Similarly, we rewrite the constraint C4 into the following form:

$$\begin{aligned} t_3^l[n] + t_4^l[n] - \frac{t_4^l[n]}{s_1^l[n]}(s_1[n] - s_1^l[n]) \\ - \frac{(2t_3^l[n] + t_4^l[n])}{s_2^l[n]}(s_2[n] - s_2^l[n]) \leq \gamma, \end{aligned} \quad (16)$$

where $t_3^l[n] = \frac{P_{URU}^* D_3^2}{(s_2^l[n])^2}$ and $t_4^l[n] = \frac{P_{LRU}^* D_4^2}{s_1^l[n]s_2^l[n]}$.

As a result, substituting (15) and (16) into (14) yields

$$\begin{aligned} & \underset{\{\mathbf{q}_r[n], h_r[n], s_1[n], s_2[n]\}}{\text{maximize}} \quad \frac{1}{N} \sum_{n=1}^N \left[t_1^l[n] + t_2^l[n] - \frac{t_2^l[n]}{s_2^l[n]}(s_2[n] - s_2^l[n]) \right. \\ & \quad \left. - \frac{(2t_1^l[n] + t_2^l[n])}{s_1^l[n]}(s_1[n] - s_1^l[n]) \right] \\ & \text{s.t.} \quad C1 \sim C3, \\ & \quad (16), (1). \end{aligned} \quad (17)$$

The problem (17) is convex and can be efficiently tackled by the interior-point method [2], [3].

C. Overall algorithm

The overall algorithm for the joint optimization of (5) is summarized in Algorithm 1. Since the variables $\Phi[n]$ and $\{\mathbf{q}_r[n], h_r[n]\}$ are updated alternately, Algorithm 1 is non-decreasing over iterations and converges to a stationary point; the relevant details can be found in [2], [3]. Furthermore, in each iteration of Algorithm 1, the subproblems defined in (10) and (17) are sequentially optimized using the existing standard convex solvers, and thus their individual complexity can be denoted by $\mathcal{O}[N(M)^{4.5}]$ and $\mathcal{O}[(N)^{3.5}]$, respectively. The symbol N and M represent the numbers of time slots and reflection elements, respectively. Thus, the total complexity of overall algorithm in Algorithm 1 is $\mathcal{O}[N_{ite}N(M)^{4.5}]$, where N_{ite} indicates the numbers of required iterations.

IV. SIMULATION RESULTS

In this section, we validate the secure sensing performance of the proposed UAV-mounted RIS-aided joint design scheme. The simulation parameters are set as follows. The initial and final coordinates of the UAV are

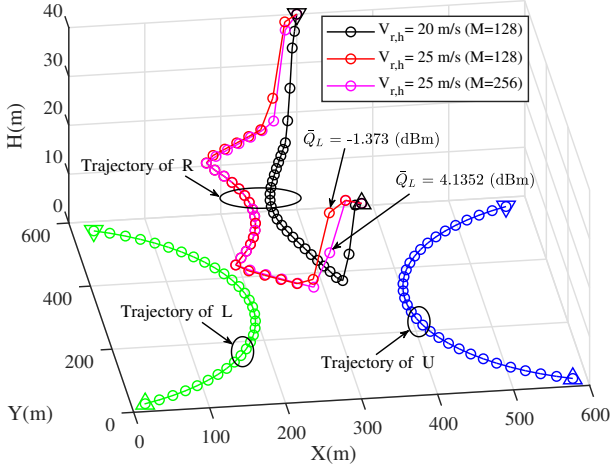
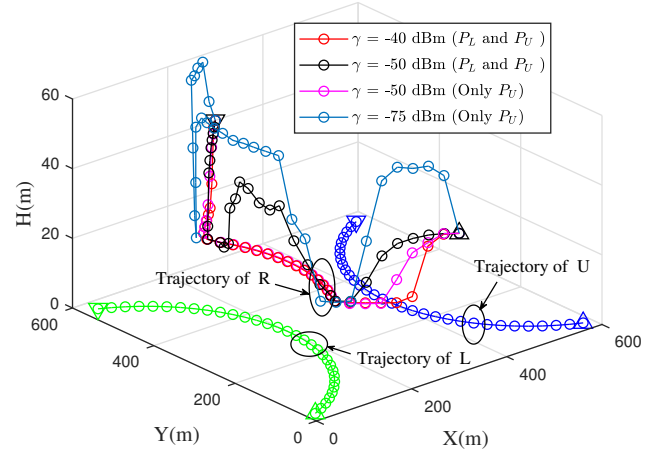


Fig. 2: UAV trajectories with different $V_{r,h}$ and M .

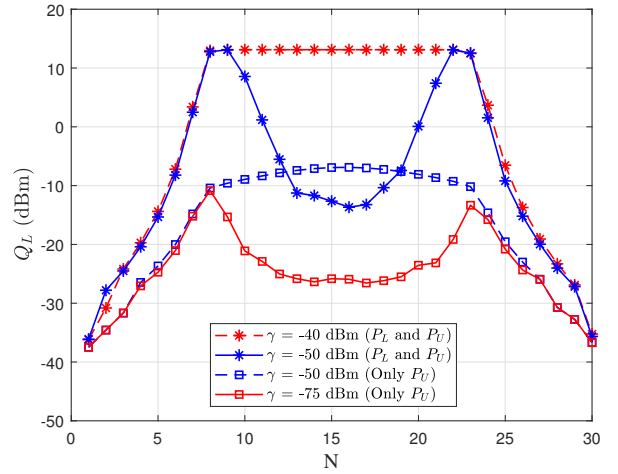
located at $(x_r[0], y_r[0], h_r[0]) = (300, 0, 40)$ m and $(x_r[N], y_r[N], h_r[N]) = (300, 600, 40)$ m, respectively. In addition, unless stated otherwise, we set $N = 30$, $M = 128$, $M_L = M_U = 40$ [16], $\gamma = -40$ dBm, $\beta_0 = -20$ dB, $d = \lambda/2$, $P_L = P_U = 1.25$ W, $V_{r,h} = 20$ m/s, $V_{r,v} = 20/\sqrt{2}$ m/s, $h_s = 20$ m and $h_l = 60$ m, respectively [2], [3].

Fig. 2 plots the collaborative UAV's flight trajectories versus different horizontal speeds $V_{r,h}$ and numbers of reflection elements M , respectively. The initial and final locations of the L/U and R are set as \triangle and ∇ , respectively. From Fig. 2, when $V_{r,h} = 20$ m/s, we notice that the UAV R almost directly moves to the final location due to the minimum flight time N constraint. However, when $V_{r,h}$ increases, the UAV target can adjust its flight route to move away from the U while approaching the L as close as possible to improve the secure sensing performance. Moreover, when M increases, i.e., $M = 256$, the average received power \bar{Q}_L is large and the UAV's flight trajectory remains the same. The reason is that the UAV target can always keep the optimal routes to maximize the received power at the L when the secure sensing threshold γ is sufficiently large.

Fig. 3(a) depicts the UAV's flight trajectories versus different γ thresholds and sensing scenarios, where it is assumed that either both L and U transmit the sensing signals or only U emits signals. As can be seen in Fig. 3(a), when γ decreases in both cases, the UAV target must ascend to a higher flight altitude to evade detection by the unauthorized shipborne radar U. Moreover, as shown in Fig. 3(b), when both L and U transmit radar pulses, i.e., both P_L and P_U are present, the L can obtain a higher received signal power in general compared to the case where only P_U is present. The reason is that the RIS can simultaneously reflect the sensing signals from L and U. In addition, it is noticed that when γ is small, i.e., $\gamma = -50$ dBm (P_L and P_U) and $\gamma = -75$ dBm (only P_U), the received signal power of L decreases rapidly in some time slots. This is because in these slots, the UAV target needs to climb the flight altitude to steer away from



(a)



(b)

Fig. 3: (a) UAV trajectories with different values of γ ; (b) Received signal power with different values of γ .

the detection of U, and thereby reduces the reflected signal powers to L.

Fig. 4 compares the received power gain of the proposed scheme with the following benchmark approaches: 1) The fixed RIS phase shift scheme (denoted as FRPS scheme), where the RIS phase shift is set as the initial optimal phase shift, i.e., $\theta_m[n] = \theta_m^*[0]$; 2) The fixed UAV flight trajectory scheme (denoted as FUFT scheme), where the UAV follows the pre-planned straight-line trajectory, i.e., $(x_r[n], y_r[n], h_r[n]) = (300, [0, 300], 40)$ m. From the Fig. 4, we observe that the proposed scheme outperforms both the FRPS and FUFT schemes. Moreover, it is also noticed that the proposed scheme yields about 29.5 dB received power gain over the FUFT scheme. This implies that only optimizing target-mounted RIS's phase shift (e.g., terrestrial scheme) will not provide a high-level of secure detection performance to the maritime mobile sensing case.

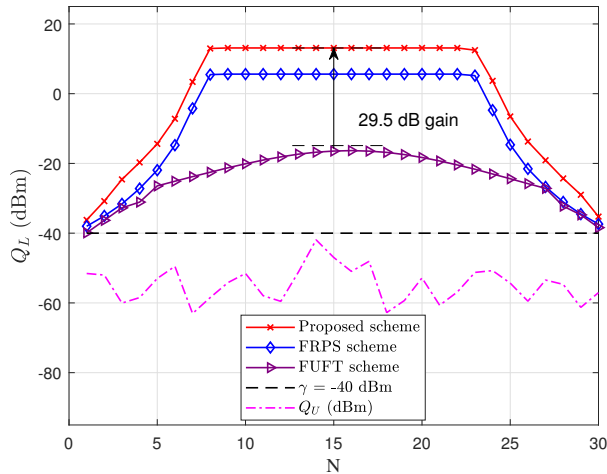


Fig. 4: Received signal power at L with different algorithms.

V. CONCLUSIONS

In this paper, we proposed a novel maritime secure sensing approach to enhance or prevent its detection by mounting the RIS on the collaborative UAV. In the proposed scheme, the RIS reflecting phase shifts and the UAV flight trajectory were designed jointly to maximize the received power at the legitimate shipborne radar while keeping the received power at the unauthorized shipborne radar below a certain level. Simulation results confirmed the effectiveness and showed the capability of the proposed scheme in the maritime secure sensing via UAV-mounted RIS.

REFERENCES

- [1] N. Nomikos, P. K. Gkonis, P. S. Bithas, and P. Trakadas, "A survey on UAV-aided maritime communications: Deployment considerations, applications, and future challenges," *IEEE Open J. Commun. Soc.*, vol. 4, pp. 5678, Jan. 2023.
- [2] L. Wu et al., "UAV-assisted maritime legitimate surveillance: Joint trajectory design and power allocation," *IEEE Trans. Veh. Technol.*, vol. 72, no. 10, pp. 13701-13705, Oct. 2023.
- [3] W. Wang et al., "Robust 3D-trajectory and time switching optimization for dual-UAV-enabled secure communications," *IEEE J. Sel. Areas Commun.*, vol. 39, no. 11, pp. 3334-3347, Nov. 2021.
- [4] H. Shin et al., "Shape optimization of an integrated mast for RCS reduction of a stealth naval vessel," *Applied Sciences*, vol. 6, no. 11, pp. 2819, Mar. 2021.
- [5] C. Wang et al., "Radar stealth and mechanical properties of a broadband radar absorbing structure," *Composites Part B: Engineering.*, vol. 123, pp. 19-27, Aug. 2017.
- [6] E. Giusti, M. Martorella, A. Capria, et al., "Electronic countermeasure for OFDM-based imaging passive radars," *2018 International Conference on Radar (RADAR), Brisbane., QLD, Australia, 2018*, pp. 1-4.
- [7] X. Shao, C. You and R. Zhang, "Intelligent reflecting surface aided wireless sensing: Applications and design issues," *IEEE Wireless Commun.*, vol. 31, no. 3, pp. 383-389, Jun. 2024.
- [8] X. Zhang and S. Song, "Secrecy analysis for IRS-aided wiretap MIMO communications: Fundamental limits and system design" *IEEE Trans. Inf. Theory*, vol. 70, no. 6, pp. 4140-4159, Jun. 2024.
- [9] J. Zhang, W. Lu, C. Xing, et al., "Intelligent integrated sensing and communication: A survey," *Sci. China Inf. Sci.*, vol. 68, no. 3, pp. 131301:42, Mar. 2025.
- [10] S. Buzzi, E. Grossi, M. Lops, and L. Venturino, "Foundations of MIMO radar detection aided by reconfigurable intelligent surfaces," *IEEE Trans. Signal Process.*, vol. 70, pp. 17491763, Mar. 2022.

- [11] K. Meng, Q. Wu, R. Schober and W. Chen, "Intelligent reflecting surface enabled multi-target sensing," *IEEE Trans. Commun.*, vol. 70, no. 12, pp. 8313-8330, Dec. 2022.
- [12] Z. Xing, R. Wang, and X. Yuan, "Joint active and passive beamforming design for reconfigurable intelligent surface enabled integrated sensing and communication," *IEEE Trans. Commun.*, vol. 71, no. 4, pp. 24572474, Apr. 2023.
- [13] C. Liao, F. Wang and V. K. N. Lau, "Optimized design for IRS-assisted integrated sensing and communication systems in clutter environments," *IEEE Trans. Commun.*, vol. 71, no. 8, pp. 4721-4734, Aug. 2023.
- [14] M. Hua, Q. Wu, W. Chen, et al., "Secure intelligent reflecting surface-aided integrated sensing and communication," *IEEE Trans. Wireless Commun.*, vol. 23, no. 1, pp. 575591, Jan. 2024.
- [15] P. Wang, W. Mei, J. Fang and R. Zhang, "Target-mounted intelligent reflecting surface for joint location and orientation estimation," *IEEE J. Sel. Areas Commun.*, vol. 41, no. 12, pp. 3768-3782, Dec. 2023.
- [16] X. Shao and R. Zhang, "Target-mounted intelligent reflecting surface for secure wireless sensing," *IEEE Trans Wireless Commun.*, vol. 23, no. 8, pp. 9745-9758, Aug. 2024.
- [17] A. M.-C. So, J. Zhang and Y. Ye, "On approximating complex quadratic optimization problems via semidefinite programming relaxations," *Mathematical Programming*, vol. 110, no. 1, pp. 93110, Jun. 2007.
- [18] M. Grant and S. Boyd, *CVX: Matlab Software for Disciplined Convex Programming*, Jul. 2010 [Online]. Available: <http://cvxr.com/cvx>.